J1.3

GENERATING INITIAL CONDITIONS FOR ENSEMBLE FORECASTS: MONTE-CARLO VS. DYNAMIC METHODS

Thomas M. Hamill[1], Jeffrey S. Whitaker[1], and Chris Snyder[2]

[1]*NOAA-CIRES Climate Diagnostics Center, Boulder, Colorado*
[2]*National Center for Atmospheric Research, Boulder, Colorado*

1. INTRODUCTION

Though ensemble forecasting has been operational in the U.S., Europe, and Canada for nearly a decade now, no clear consensus has yet evolved on the best feasible method for generating initial conditions for these ensemble forecasts. In principle, to be consistent with the underlying theory stemming from the Liouville equation (Ehrendorfer 1994), the samples, whether they are drawn randomly or non-randomly, should reflect the probability distribution of plausible analysis states. However, analysis error statistics are highly flow-dependent, and generating such flow-dependent sets of initial conditions is at best computationally very expensive. As a consequence, each of the operational centers have embraced different approaches. The European Centre for Medium-Range Weather Forecasts (ECMWF) have used "singular vector" perturbations (Molteni et al. 1996); the National Centers for Environmental Prediction (NCEP) use a "breeding" method (Toth and Kalnay 1993, 1997); and at the Canadian Meteorological Centre (CMC), a "perturbed observation" 3-dimensional variational assimilation (3D-Var) approach is used (Houtekamer et al. 1996). All of these methods can only approximate generating samples from the distribution of analysis states. In the case of ECMWF's singular vectors, in principle the initial norm used to measure the size and structure of perturbations should be a flow-dependent analysis-error covariance norm ("AEC"; more later on this); lacking that, ECMWF uses an initial total-energy norm. For NCEP's breeding method, perturbations are grown and rescaled each analysis cycle, their rescaled size consistent with time-averaged analysis error statistics. Hence, there is limited freedom for them to fully reflect the flow-dependent uncertainty. The CMC perturbed initial conditions, as shown in Hamill et al. (2000) can potentially do a good job of reflecting situational analysis errors, but some compromises are made operationally to lower the computational cost at the expense of some flow dependency.

Understanding of the relative merits of various approaches are difficult since each forecast center uses a different forecast model, different data assimilation approaches, even somewhat different sets of observations. Anderson (1996, 1997) provided some comparisons of different approaches using the 3-dimensional Lorenz (1963) model. Hamill et al. (2000) provided a comparison of singular vector, bred, and perturbed observation methods in a quasi-geostrophic channel model with O(10^5) degrees of freedom.

Some work has been done on understanding the properties of perturbations that are consistent with AECs, notably Ehrendorfer and Tribbia (1997) and Barkmeijer et al. (1998, 1999). Ehrendorfer and Tribbia (1997) showed that in principle, if one's intent is to explain forecast variance optimized for a given lead time with as little error as possible, optimally growing perturbations, or singular vectors (SVs) consistent with analysis-error covariances are the theoretically appropriate choice. However, one must develop perturbations to maximize forecast variance for a specific lead time, say, 48 h. Perhaps the structures for 24 h are somewhat different, and the optimality is only valid for a specific time, and under restrictive assumptions of linearity and Gaussianity. Barkmeijer et al.'s work also addressed the optimality of AEC SV's. In their study, they calculated the singular vectors consistent with static, non-flow dependent analysis error statistics and compared the accuracy of subsequent probabilistic forecasts against those from total-energy norm SVs (TESVs). Probabilistic forecasts from TESVs were found to be slightly more skillful than those from AEC SVs. The exact reasons were unclear, but certainly one possible reason is that the AECs used in that study were not flow dependent.

What has yet to be explored in a complex system is a comparison of probabilistic forecast errors from random and dynamically structured perturbations *both of which are consisent with flow-dependent analysis errors statistics*. We now have the tools in place to perform this comparison. Recent improvements in computational power have permitted the exploration of ensemble-based data assimilation approaches which may be able to provide not only dramatically improved analyses but flow-dependent initial conditions for ensembles (see, e.g., Evensen 1994, Houtekamer and Mitchell 1998, 2001, Burgers et al. 1998, Hamill et al. 2001, Whitaker and Hamill 2001). The general idea is this: first, run a very large ensemble-based data assimilation scheme (here, in a perfect-model context). The analyses from these schemes can be shown to be reliable and have flow-

* The National Center for Atmospheric Research is sponsored by the National Science Foundation

Corresponding author address: Dr. Thomas M. Hamill, NOAA-CIRES CDC, R/CDC 1, 325 Broadway, Boulder, CO 80305-3328. e-mail: hamill@cdc.noaa.gov

dependent error statistics. We will demonstrate that by using this ensemble, one can also determine without use of tangent-linear and adjoint models just which initial analysis-error structures, the AEC SVs, result in the largest forecast errors. We will then generate forecasts from the random and singular-vector initial conditions and compare the accuracy of the subsequent probabilistic forecasts. This preprint will primarily document the experimental design; results will be presented at the conference.

Here, we will start with a brief description of the ensemble data assimilation methodology (Section 2), the methodology for generating flow-dependent AEC SVs (Section 3), the details of our experiment and test methodology (Section 4), and results (Section 5).

2. ENSEMBLE-BASED DATA ASSIMILATION METHODOLOGY

The assimilation scheme used here has been dubbed the ensemble square-root filter, or "EnSRF." A more complete description of it and the rationale for its use is provided in Whitaker and Hamill (2001). The underlying notion is to run an ensemble of parallel forecast and data assimilation cycles, ensuring that the ensemble mean analysis and the analysis-error covariance as estimated by the ensemble is consistent with that predicted by Kalman-filter theory.

Following the notation of Ide et al. (1997), let $\mathbf{x}^b$ be a background model forecast, $\mathbf{y}^o$ be a set of observations, $\mathbf{H}$ be an operator that converts the model state to the observation space, $\mathbf{P}^b$ be the background-error covariance matrix, and $\mathbf{R}$ be the observational-error covariance matrix. The minimum error variance estimate of the analyzed state $\mathbf{x}^a$ is then given by the traditional Kalman filter update equation (Lorenc 1986),

$$\mathbf{x}^a = \mathbf{x}^b + \mathbf{K}(\mathbf{y}^o - \mathbf{H}\mathbf{x}^b), \tag{1}$$

where

$$\mathbf{K} = \mathbf{P}^b\mathbf{H}^T(\mathbf{H}\mathbf{P}^b\mathbf{H}^T + \mathbf{R})^{-1}. \tag{2}$$

The expected analysis-error covariance is

$$\mathbf{P}^a = (\mathbf{I} - \mathbf{K}\mathbf{H})\mathbf{P}^b. \tag{3}$$

In the generic ensemble Kalman filter (EnKF; Evensen 1994, Houtekamer and Mitchell 1998, Burgers et al. 1998, Hamill et al. 2001), $\mathbf{P}^b$ is approximated using the sample covariance from an ensemble of model forecasts; $\mathbf{P}^b = \langle \mathbf{x}'^b\mathbf{x}'^{bT} \rangle$, where $\langle \cdot \rangle$ denotes the expected value, computed using the ensemble. In actuality, there is no need to compute and store the full matrix $\mathbf{P}^b$. Instead, matrices $\mathbf{P}^b\mathbf{H}^T$ and $\mathbf{H}\mathbf{P}^b\mathbf{H}^T$ are estimated directly using the ensemble (Evensen 1994, Houtekamer and Mitchell 1998).

The update equations can be re-expressed in separate equations for the ensemble mean (denoted by an overbar) and a deviation from the mean (denoted by a prime):

$$\overline{\mathbf{x}}^a = \overline{\mathbf{x}}^b + \mathbf{K}(\mathbf{y}^o - \mathbf{H}\overline{\mathbf{x}}^b), \tag{4}$$

$$\mathbf{x}'^a = (\mathbf{I} - \widetilde{\mathbf{K}}\mathbf{H})\mathbf{x}'^b. \tag{5}$$

Here, $\mathbf{K}$ is the traditional Kalman gain given by Eq. (2), and $\widetilde{\mathbf{K}}$ is the gain used to update deviations from the ensemble mean.

When sequentially processing independent observations, $\mathbf{K}$, $\widetilde{\mathbf{K}}$, $\mathbf{H}\mathbf{P}^b$ and $\mathbf{P}^b\mathbf{H}^T$ are all vectors with the same length as the model state vector, and $\mathbf{H}\mathbf{P}^b\mathbf{H}^T$ is a scalar. Thus, as first noted by Potter (1964), when observations are processed one at a time,

$$\widetilde{\mathbf{K}} = \left(1 + \sqrt{\frac{\mathbf{R}}{\mathbf{H}\mathbf{P}^b\mathbf{H}^T + \mathbf{R}}}\right)^{-1} \mathbf{K}. \tag{6}$$

Here, $\mathbf{H}\mathbf{P}^b\mathbf{H}^T$ and $\mathbf{R}$ are scalars representing the background and observational error variance at the observation location. The quantity multiplying $\mathbf{K}$ in Eq. (11) is a scalar between 0 and 1. This means that, in order to obtain the desired analysis-error covariance, one uses a modified Kalman gain to update deviations from the ensemble mean that is reduced in magnitude relative to the traditional Kalman gain. Thus, deviations from the mean are reduced less in the analysis using $\widetilde{\mathbf{K}}$ than they would be using $\mathbf{K}$. In the EnKF, the excess variance reduction caused by using $\mathbf{K}$ to update deviations from the mean is compensated for by the introduction of noise to the observations. In the EnSRF, the mean and departures from the mean are updated independently according to Eqs. (4) and (5). If observations are processed one at a time, the EnSRF requires no more computation than the traditional EnKF with perturbed observations.

The general analysis methodology is thus as follows: generate a set of perturbed initial conditions. Make n forecasts forward to the next data assimilation time. Perform $n+1$ parallel data assimilation cycles, updating the mean state using (4) and the n perturbations using (5) and (6). In each data assimilation cycle, observations are assimilated serially.

Some additional algorithmic complexity will be used in order to model background-error covariances more effectively. These include the inflation and localization of covariances. Deviations of perturbations of each member from the ensemble mean are inflated by a small amount before the start of each data assimilation cycle in order to ensure that covariances are not systematically underestimated, which can cause a problem known as filter divergence, whereby the influence of new observations is ignored. Covariance localization multiplies the ensemble estimate of covariances with an isotropic function which monotonically decreases with greater distance from the observation. See Hamill et al. (2001) for an in-depth rationale and mathematical formalism.

3. ANALYSIS-ERROR COVARIANCE SINGULAR VECTORS USING ENSEMBLES

Let $\mathbf{X}_a = (n-1)^{-1/2}(\mathbf{x}_1^{\mathrm{a}} - \overline{\mathbf{x}}^{\mathrm{a}}, \ldots, \mathbf{x}_n^{\mathrm{a}} - \overline{\mathbf{x}}^{\mathrm{a}})$, where the ith column vector represents the ith member $\mathbf{x}_i^{\mathrm{a}}$'s analyzed model state deviation from the ensemble mean analysis $\overline{\mathbf{x}}^{\mathrm{a}}$. We assume that the ensemble samples analysis errors correctly, so that

$$\lim_{n\to\infty} \mathbf{X}_a \mathbf{X}_a{}^{\mathrm{T}} = \mathbf{P}^{\mathrm{a}} \tag{7}$$

We also assume linear dynamics. Let $\mathbf{M}$ denote the tangent-linear operator of the forecast model. Under assumptions of linearity we can construct an ensemble of forecast deviations from the ensemble mean according to

$$\begin{aligned}\mathbf{X}_f &= (n-1)^{1/2}\left(\mathbf{x}_1^{\mathrm{f}} - \overline{\mathbf{x}}^{\mathrm{f}}, \ldots, \mathbf{x}_n^{\mathrm{f}} - \overline{\mathbf{x}}^{\mathrm{f}}\right) \\ &\simeq (n-1)^{1/2}\left(\mathbf{M}(\mathbf{x}_1^{\mathrm{a}} - \overline{\mathbf{x}}^{\mathrm{a}}), \ldots, \mathbf{M}(\mathbf{x}_n^{\mathrm{a}} - \overline{\mathbf{x}}^{\mathrm{a}})\right) \\ &\simeq \mathbf{M}\mathbf{X}_a .\end{aligned}$$

So

$$\lim_{n\to\infty} \mathbf{X}_f \mathbf{X}_f{}^{\mathrm{T}} = \mathbf{M}\mathbf{X}_a \mathbf{X}_a^{\mathrm{T}} \mathbf{M}^{\mathrm{T}} \tag{8}$$

With the same generality, $\mathbf{X}_f$ can be estimated from an ensemble of nonlinear forecasts:

$$\mathbf{X}_f \simeq (n-1)^{1/2}\left(M(\mathbf{x}_1^{\mathrm{a}}) - \overline{M(\mathbf{x}^{\mathrm{a}})}, \ldots, M(\mathbf{x}_n^{\mathrm{a}}) - \overline{M(\mathbf{x}^{\mathrm{a}})}\right)$$

where $\overline{M(\mathbf{x}^{\mathrm{a}})} = n^{-1}\sum_{i=1}^{n} M(\mathbf{x}_i^{\mathrm{a}})$.

Let us denote an energy inner product with norm $|\mathbf{x}| = \mathbf{x}^{\mathrm{T}}\mathbf{S}\mathbf{x} = (\mathbf{D}\mathbf{x})^{\mathrm{T}}(\mathbf{D}\mathbf{x})$, where $\mathbf{D} = \mathbf{S}^{1/2}$, and $\mathbf{D}$ is symmetric, i.e., $\mathbf{D} = \mathbf{D}^{\mathrm{T}}$. To find analysis-error covariance singular vectors, we would like to maximize forecast deviations, measured in a total-energy norm, subject to the constraint that the initial perturbations are sized to be consistent with the analysis-error statistics, i.e.,

$$max \ \frac{\mathbf{X}_f^{\mathrm{T}}\mathbf{S}\mathbf{X}_f}{\mathbf{X}_a^{\mathrm{T}}\mathbf{P}^{\mathrm{a}-1}\mathbf{X}_a^{\mathrm{T}}}$$

or

$$max \ \frac{\mathbf{X}_a^{\mathrm{T}}\mathbf{M}^{\mathrm{T}}\mathbf{S}\mathbf{M}\mathbf{X}_a}{\mathbf{X}_a^{\mathrm{T}}\mathbf{P}^{\mathrm{a}-1}\mathbf{X}_a},$$

which, by Rayleigh's principle, is equivalent to the eigenvalue problem

$$\mathbf{M}^{\mathrm{T}}\mathbf{S}\mathbf{M}\mathbf{u} = \mathbf{P}^{\mathrm{a}-1}\mathbf{u}\lambda \tag{9}$$

where $\mathbf{u}$ denotes the eigenvector and λ the associated eigenvalue. Multiplying both sides by $\mathbf{D}\mathbf{M}\mathbf{P}^{\mathrm{a}}$ and substituting $\mathbf{D}^2$ for $\mathbf{S}$, this yields

$$\mathbf{D}\mathbf{M}\mathbf{P}^{\mathrm{a}}\mathbf{M}^{\mathrm{T}}\mathbf{D}^2\mathbf{M}\mathbf{u} = \mathbf{D}\mathbf{M}\mathbf{u}\lambda \tag{10}$$

Letting $\mathbf{d} = \mathbf{D}\mathbf{M}\mathbf{u}$, and assuming

$$\lim_{n\to\infty} (\mathbf{D}\mathbf{X}_f)(\mathbf{D}\mathbf{X}_f)^{\mathrm{T}} = \mathbf{D}\mathbf{P}^{\mathrm{f}}\mathbf{D}$$

(10) then becomes

$$\mathbf{D}\mathbf{M}\mathbf{P}^{\mathrm{a}}\mathbf{M}^{\mathrm{T}}\mathbf{D}\mathbf{d} = \mathbf{D}\mathbf{P}^{\mathrm{f}}\mathbf{D}\mathbf{d} = \mathbf{D}\mathbf{X}_f(\mathbf{D}\mathbf{X}_f)^{\mathrm{T}}\mathbf{d} = \mathbf{d}\lambda \tag{11}$$

an equivalent eigenvalue problem for the forecasts. Here, $\mathbf{d}$'s are the eigenvectors of the forecast covariance matrix in a norm based on $\mathbf{S} = \mathbf{D}^2$. Now, let $\mathbf{d} = \mathbf{D}\mathbf{X}_f\alpha$, i.e., α is an n-dimensional vector with elements representing the weight to be given to each column of $\mathbf{D}\mathbf{X}_f$. Then, substituting this definition, using the identity $(\mathbf{D}\mathbf{X}_f)^{\mathrm{T}} = \mathbf{X}_f^{\mathrm{T}}\mathbf{D}^{\mathrm{T}}$ and eliminating a $\mathbf{D}\mathbf{X}_f$ from each side, one can show that an equivalent eigenvalue problem to (11) is

$$\mathbf{X}_f^{\mathrm{T}}\mathbf{D}^{\mathrm{T}}\mathbf{D}\mathbf{X}_f\alpha = \alpha\lambda$$

for $\lambda \neq 0$. Next, assuming $\mathbf{X}_f = \mathbf{M}\mathbf{X}_a$ and $\mathbf{S} = \mathbf{D}^{\mathrm{T}}\mathbf{D}$,

$$\mathbf{X}_a^{\mathrm{T}}\mathbf{M}^{\mathrm{T}}\mathbf{S}\mathbf{M}\mathbf{X}_a\alpha = \alpha\lambda.$$

Multiplying both sides by $\mathbf{X}_a$ and using (1), for an infinite ensemble

$$\mathbf{P}^{\mathrm{a}}\mathbf{M}^{\mathrm{T}}\mathbf{S}\mathbf{M}\mathbf{X}_a\alpha = \mathbf{X}_a\alpha\lambda. \tag{12}$$

Assuming $\mathbf{u} = \mathbf{X}_a\alpha$, this is equivalent to (9). In plainer terms, what (12) indicates is that when one has determined the eigenvectors of the forecasts using the ensemble, the same linear combination α of ensemble forecast members that yields a given forecast eigenvector can be multiplied by the analysis members to determine the associated analysis structure that gave rise to this forecast eigenvector.

Terminology may be confusing when different initial and final norms are used. The linear combination α of ensemble forecast deviations will be what we refer to as the "evolved" or "forecast" singular vectors. The same linear combination α of analysis state deviations will be referred to as the "initial time" singular vectors. Were the norms consistent, the maximum growth rate would be associated with the leading evolved singular vector. As will be shown in section 5, this is not necessarily so with the AEC SVs.

4. EXPERIMENTAL DESIGN

Aspects of our experimental design may change before the conference; we describe the setup for preliminary tests conducted so far.

We use a Held/Suarez dry, primitive equation global circulation model (Lee and Held 1993) under assumptions of no model error. The model is T31L15 resolution.

A 100-member EnSRF data assimilation system is used. Covariances are localized using a Schur

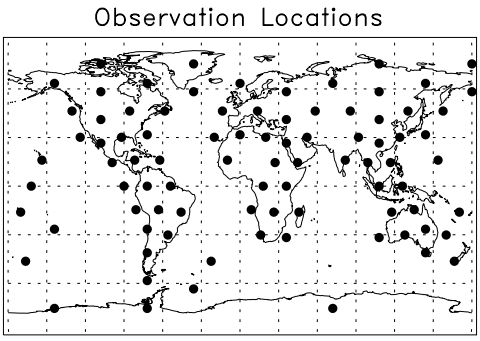

Figure 1. Locations of synthetic rawinsonde profiles.

product of ensemble covariances with a ∼Gaussian-shaped function with local support, reaching a zero value at 5000 km distance from the observation. Before each data assimilation cycle, covariances are inflated by 2 %.

Two types of observations are assimilated; the first are synthetic rawinsondes (raobs), with a surface pressure observation and winds and temperature at 5 vertical levels, approximately 900, 700, 500, 300, and 100 hPa. Observations have error characteristics derived from Parrish and Derber (1992), and observation errors are assumed uncorrelated in the vertical. Observation locations are shown in Fig. 1; they were chosen to provide a very rough analogue to the operational raob network, with more observations over the land than the ocean. Another set of observations, roughly analogous to upper cloud-drift winds, are also assimilated. These observations are randomly located in longitude, are random normally distributed about the equator with a standard deviation of 20 ° latitude, and are randomly placed in the vertical between 400 and 200 hPa. Drift error statistics are again consistent with the 6.1 ms^{-1} standard deviation cited in Parrish and Derber (1992). Analysis errors are shown in Fig. 2.

From the cycled analyses, we periodically make an ensemble of 48-h forecasts. AEC SVs are computed using Northern Hemisphere ensemble forecast data north of 20 °. The eigenvalues and eigenvectors of the forecast-error covariance are calculated and ordered. To determine the associated initial-time structure, the linear combination of ensemble forecast members that produced a given eigenvector is used, but applied to the initial-time ensemble. Under linearity assumptions, this should produce the correct initial-time structure.

5. RESULTS

A more complete set of results will be presented at the conference. Here we provide a preliminary glimpse at the properties of AEC SVs in this model.

Analysis-error statistics show that, even with the inclusion of synthetic cloud-drift winds in the tropics, the typical magnitudes of analysis errors are still dominated by wind errors in the tropical upper troposphere (Fig. 2). By generating singular vectors only using data north of 20 °, we are able to generate singular vectors that are not dominated by the low-latitude errors.

Figure 3 shows the leading forecast eigenvector and the associated initial-time structure that produced it on day 70. Several characteristics are notable; first, the structure is quite localized relative to the 3D-Var Hessian singular vectors cited in Barkmeijer et al. (1998, 1999). We have not yet computed statistics for a wide number of cases and so are unable to determine the pressure level where initial amplitudes are the largest.

At the time of the conference, we expect to have more description of the characteristics of the analysis error, the typical structures of the AEC SVs, and information on how skillful are probabilistic forecasts generated from random samples or from AEC SVs.

One interesting feature is that the amplification factors do not decrease monotonically as the singular vector number increases. For example, Fig. 4 plots the amplification factors of the singular vectors, the size of the perturbation at the final time divided by the size of the perturbation at the initial time (both measured here in a total-energy norm). Recall that the singular vectors are ordered in terms of the amount

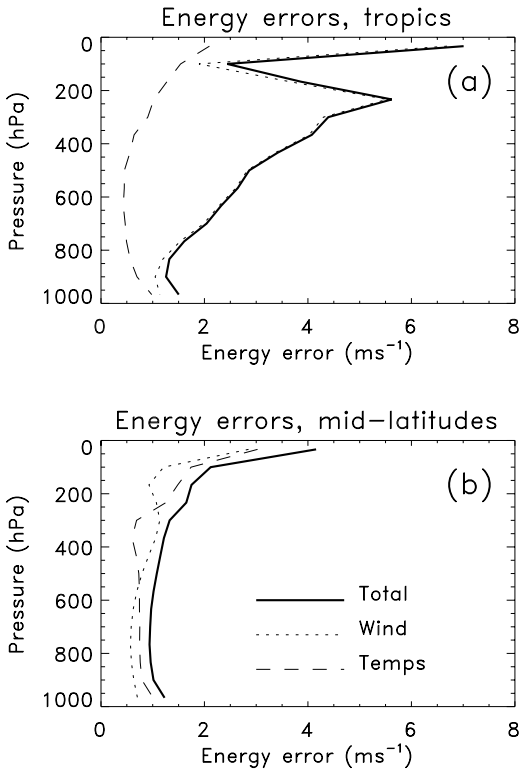

Figure 2. Energy errors for the analysis (total, wind, and temperature component) as a function of height. (a) 27.5° N to 27.5° S, and (b) north of 37.5° N latitude.

of *forecast-error* variance that they explain. Figure 4 illustrates that the amplification of the second singular vector is smaller than the third, fourth, and fifth singular vectors. This does not indicate a problem with the methodology; rather, it highlights that there are two factors contributing to the final forecast error structure; forecast errors can grow to be large either from the initial errors being large *and/or* a large growth rate during the forecast. Apparently, singular vector 2 had a large initial amplitude, compensating for its smaller growth rate.

REFERENCES

Anderson, J. L., 1996: A method for producing and evaluating probabilistic forecasts from ensemble model integrations. *J. Climate*, **9**, 1518-1530.

—— , 1997: Impact of dynamical constraints on the selection of initial conditions for ensemble predictions: low-order perfect model results. *Mon. Wea. Rev.*, **125**, 2969-2983.

Barkmeijer, J., M. van Gijzen, and F. Bouttier, 1998: Singular vectors and estimates of the analysis error covariance metric. *Quart. J. Roy. Meteor. Soc.*, **124**, 1695-1713.

—— , R. Buizza, and T.N. Palmer, 1999: 3D-Var Hessian singular vectors and their potential use in the ECMWF ensemble prediction system. *Quart. J. Roy. Meteor. Soc.*, **125**, 2333-2351.

Burgers, G., P. J. van Leeuwen, and G. Evensen, 1998: Analysis scheme in the ensemble Kalman filter. *Mon. Wea. Rev.*, **126**, 1719-1724.

Ehrendorfer, M., 1994: The Liouville equation and its potential usefulness for the prediction of forecast skill. part I: theory. *Mon. Wea. Rev.*, **122**, 703-713.

Ehrendorfer, M., and J. J. Tribbia, 1997: Optimal prediction of forecast error covariances through singular vectors. *J. Atmos. Sci.*, **54**, 286–313.

Evensen, G., 1994: Sequential data assimilation with a nonlinear quasigeostrophic model using Monte Carlo methods to forecast error statistics. *J. Geophys. Res.*, **99 (C5)**, 10143-10162.

Hamill, T. M., C. Snyder, and R. E. Morss, 2000: A comparison of probabilistic forecasts from bred, singular vector, and perturbed observation ensembles. *Mon. Wea. Rev.*, **128**, 1835-1851.

Hamill, T. M., J. S. Whitaker, and C. Snyder, 2001: Distance-dependent filtering of background error covariance estimates in an ensemble Kalman filter. *Mon. Wea. Rev.*, **129**, 2776-2790.

Houtekamer, P. L. , L. Lefaivre, and J. Derome, 1996: The RPN ensemble prediction system. *Proc. ECMWF Seminar on Predictability, Vol II*, Reading, United Kingdom, 121-146. [Available from ECMWF, Shinfield Park, Reading, Berkshire RG2 9AX, United Kingdom].

—— , and H. L. Mitchell, 1998: Data assimilation using an ensemble Kalman filter technique. *Mon. Wea. Rev.*, **126**, 796-811.

—— , and —— , 2001: A sequential ensemble Kalman filter for atmospheric data assimilation. *Mon. Wea. Rev.*, **129**, 123-137.

Ide, K., P. Courtier, M. Ghil, and A. C. Lorenc, 1997: Unified notation for data assimilation: operational,

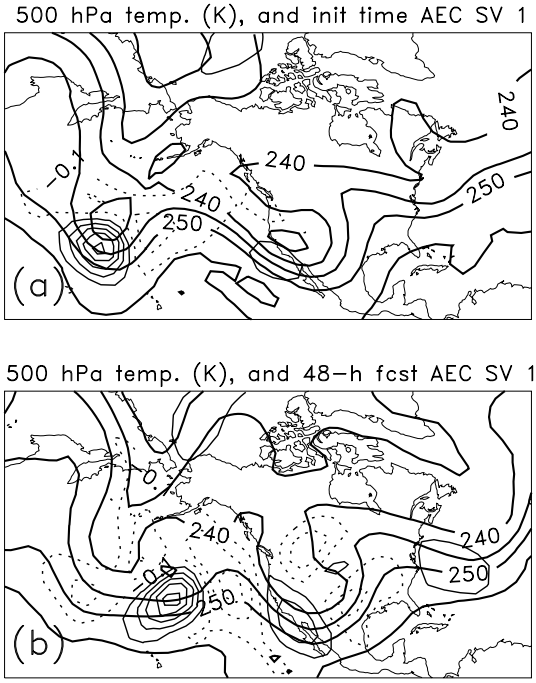

Figure 3. Analysis-error covariance singular vectors. An example, here from day 70, of (a) the ensemble-mean analysis 500 hPa temperature and the projection of the leading initial-time singular vector on 500 hPa temperature. Singular vector projections normalized by the maximum amplitude, with contours at +/- 0.1,0.3,0.5,0.7, and 0.9. Dashed indicate negative amplitudes. (b) as in (a) but the singular vectors of the evolved 48-h forecast.

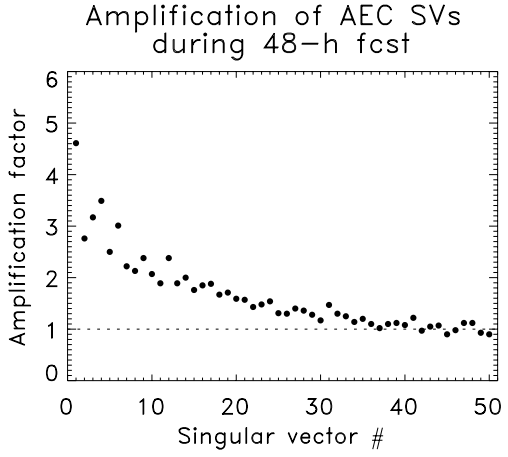

Figure 4. Amplification factors (final energy/initial energy, measured in total energy norm) of AEC SVs for day 70.

sequential, and variational. *J. Met. Soc. Japan*, **75 (1B)**, 181–189.

Lee, S., and I. M. Held, 1993: Baroclinic wave packets in models and observations. *J. Atmos. Sci.*, **50**, 1413-1428.

Lorenc, A. C., 1986: Analysis methods for numerical weather prediction. *Quart. J. Roy. Meteor. Soc.*, **112**, 1177–1194.

Lorenz, E. N., 1963: Deterministic nonperiodic flow. *J. Atmos. Sci.*, **20**, 131-140.

Molteni, F., R. Buizza, T. N. Palmer, and T. Petroliagis, 1996: The ECMWF ensemble prediction system: methodology and validation. *Quart. J. Roy. Meteor. Soc.*, **122**, 73-119.

Parrish, D. F., and J. C. Derber, 1992: The National Meteorological Center's Spectral Statistical Interpolation Analysis System. *Mon. Wea. Rev.*, **120**, 1747-1763.

Potter, J., 1964: W matrix augmentation. M.I.T. Instrumentation Laboratory Memo SGA 5-64, Massachusetts Institute of Technology, Cambridge, MA.

Toth, Z., and E. Kalnay, 1993: Ensemble forecasting at NMC: The generation of perturbations. *Bull. Amer. Meteor. Soc.*, **74**, 2317-2330.

——— , and ——— , 1997: Ensemble forecasting at NCEP and the breeding method. *Mon. Wea. Rev.*, **12**, 3297-3319.

Whitaker, J. S., and T. M. Hamill, 2001: Ensemble data assimilation without perturbed observations. *Mon. Wea. Rev.*, **129**, accepted. Available from www.cdc.noaa.gov/∼jsw .